CrossMark

ORIGINAL ARTICLE

Practical methodology for validating constitutive models for the simulation of rubber compounds in extrusion processes

Ruben Urraca[1] · Alpha Pernía-Espinoza[1] · Ismael Díaz[2] · Andres Sanz-Garcia[3]

Abstract Rubber profile manufacturers have strong incentives to optimize the design of their extrusion dies and reduce the longer development times. Computational fluid dynamics (CFD) modeling is today the most effective alternative to traditional methods for adjusting die geometry and extrusion parameters. However, in practical terms, CFD modeling is often hindered by particular features of the extrusion process such as the lack of a single constitutive equation for all types of rubber flow. This article proposes a practical methodology based on simulation results and experimental data from an easy-to-build 4-channel die to help in the selection of the most adequate constitutive model of a rubber blend. The methodology was validated in a particular ethylene-propylene-diene monomer (EPDM). Characterization experiments were first carried out to obtain three constitutive models: Herschel-Bulkley, Bird-Carreau, and power law. Then, the EPDM was extruded in the manufactured die, and the total rubber that passes through the 4-channel die together with the inlet pressure was measured. CFD simulations of the 4-channel die were lastly analyzed. In our case study, the Bird-Carreu model, experimentally obtained by dynamic mechanical analysis, turned out to be the best candidate model for the EPDM studied. Subsequently, we demonstrated that a valid constitutive equation can be effectively selected by applying the methodology proposed with relatively low cost.

Keywords Extrusion die design · Viscosity curve · Validation process · Rubber long profile · Computational fluid dynamics · Constitutive equations

Abbreviations
CAD Computer-aided design
CFD Computational fluid dynamics
FEM Finite element method
FVM Finite volume method
EPDM Ethylene-propylene-diene monomer
GNF Generalized Newtonian fluid
DMA Dynamic mechanical analysis

1 Introduction

Long rubber profiles with heterogeneous cross-section shapes are traditionally installed in the opening and shutting parts of vehicles, such as windows, doors, or trunks [1]. They reduce noise and vibrations, as they seal the vehicle and also prevent air and water from getting into the cab. Nowadays, the automobile industry demands that long profile manufacturers meet extremely high-quality standards [2]. Profiles that do not fulfill the strict requirements must be discarded, reducing the production rate [3]. Besides, with today's ever-changing global markets, new vehicle models are debuting on the market at an extremely fast rate, enforcing profile manufacturers to reduce design times and optimize their extrusion processes [4].

Die design and fabrication clearly lack of automation and current methods mainly relies on a trial-and-error basis

✉ Andres Sanz-Garcia
andres.sanz-garcia@helsinki.fi

1 Department of Mechanical Engineering, University of La Rioja, Logroño, Spain

2 Standard Profil, S.A, Logroño, Spain

3 Division of Pharmaceutical Biosciences, University of Helsinki, Viikinkaari 5 E (P.O. Box 56), 00014 Helsinki, Finland

influenced by previous experiences [5]. When an automotive company demands a new profile, the geometry of the extrusion die is first designed by using computer-aided design (CAD) tools [6]. However, given only the die geometry, designers do not have a direct means of verifying profile's quality and final shape [7]. Therefore, once the extrusion die is machined according to the initial digital design, repeated extrusion trials and manual die modifications are carried out to give experts better guidance to file down or add material to different passages of the plates that form the die. In case of commercial profiles, more than a dozen cycles are required before the desired profile is produced, which increase costs and create extended periods of time to start the mass production [8]. Moreover, the success of this adjustment strongly relies on the designers' technical qualification and experience [9].

This time-consuming adaptation process can be shortened by using computer simulations of rubber extrusion dies [10, 11] that replace physical extrusion trials [12]. The computational models developed can be used not only to predict product's final geometry [13] but also to enclose within an optimization framework that helps in the adjustment of die dimensions [14, 15]. In this context [16], a wide variety of modeling approaches has been already tested [17]. Analytical formulas were the first models used to predict different parameters of the rubber extrusion process [18, 11]. Data-driven-based models have also been used to estimate the flow behavior [9, 14], but simulations based on computational fluid dynamics (CFD) are the most effective tool for modeling extrusion processes [19]. CFD models are based on the physical principles underlying the extrusion process [20]. An approximate solution of the system of governing equations can be obtained using numerical procedures such as the finite element method (FEM) [3] or the finite volume method (FVM) [21]. Both approaches assure the accuracy and repeatability of the simulation results; however, the number of published works where complex commercial extrusion dies are simulated is relatively low. Some exceptions are the works of del Coz Díaz et al. [22, 23] showing acceptable results but with weak validation processes based on velocity profiles. In addition, research on novel CFD codes has tended to focus on easier scenarios with profiles of simple cross section rather than working with the complex geometry of commercial profiles [24] [25]. Other research works have simulated the evolution of the rubber flow only in a specific part of the die such as the land plate [26], and even in some cases, CFD simulations were performed in a two-dimensional (2D) domain [27, 28].

The simulation of extrusion dies of commercial rubber profiles still represents a challenge seldom embraced mainly due to the existing convergence issues and the lack of experimental data. This paper copes both problems by analyzing the viscous

constitutive equations of rubber compounds [29]. The constitutive equation relates the applied shear stress (τ) with the shear rate ($\dot{\gamma}$) by means of the apparent viscosity (η). Determining the correct constitutive equation is not a univocal process. The viscous part of the equation could be modeled from a simple Newtonian model to highly complex non-Newtonian approaches such as the power law, Bird-Carreau, Herschel-Bulkley, and Carreau-Yasuda. The elastic part may be also taken into account when working with some complex phenomena such as the die swell [30–32]. Elastic behavior could be modeled using equations such as the upper-convected Maxwell and Oldroyd-B model. Moreover, variations in viscosity through different melting temperatures can be significant under some specific conditions, so it has to be accounted using Arrhenius, Fulcher, or Williams-Landel-Ferry laws.

The selection of the equipment required for the experimental tests is not a direct decision. Rubber compounds present significant higher viscosity values than other traditional fluids simulated by CFD [12]. In some cases, several experiments are required prior to select the rheometer whose operating conditions are closer to the real process [33]. Therefore, both the constitutive equation that better capture the behavior of the rubber and the experimental procedure required for determining its parameters are difficult to select a priori. This situation usually generates a considerable uncertainty regarding the material behavior and also in the CFD simulation results. Ensuring the right constitutive equation will not only remove a critical factor that may lead CFD simulations to divergence but also will help in model validation purposes.

This paper tackles the aforementioned issues from a practical point of view. Using a commercial FE package and an easy-to-build 4-channel extrusion die, we propose a methodology to validate constitutive models obtained from rheological characterization for rubber compounds. The methodology was validated with an ethylene-propylene-diene monomer (EPDM) produced by Standard Profil S.A. (labeled as EPDM-917). This methodology might be implemented for helping in the creation of more reliable CFD models of the rubber extrusion dies. Our ultimate goal is to promote the adoption of CFD modeling techniques in the manufacture of rubber profiles as well as boosting the automation of die design processes.

2 Description of the methodology proposed

A practical methodology is presented to help in the selection of the constitutive model that represents better the rubber blend behavior on a particular extrusion process, such as the one in Fig. 1a. The methodology allows us to select the most adequate constitutive equation every time a new rubber blend is included in production. We create a simplified scenario using a non-commercial 4-channel extrusion die detailed in Figs. 1b–d, where a series of numerical simulations with different
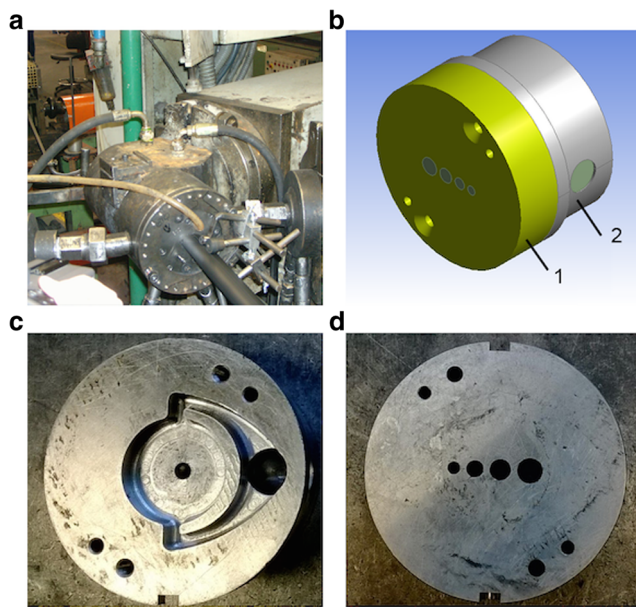
Fig. 1 General overview of a rubber profile leaving the plate die in the extrusion line (**a**) and the proposed 4-channel die: CAD design (**b**), extruder mounting plate (**c**), and die land plate (**d**)

constitutive equations can be easily performed within an acceptable time [34]. This methodology is divided into four steps:

1. To carry out a series of experiments where the new compound is extruded in the 4-channel die. The total flow that leaves each channel is measured.
2. To determine the potential constitutive equations of the compound. These are obtained experimentally following different characterization approaches.
3. To perform numerical simulations of the fluid going through the 4-channel die using the constitutive equations determined in step 2.
4. To compare the results of the numerical simulations against the experimental data. The constitutive equation of the simulation which results gets closer to the experimental values is selected as the best candidate for simulating the compound on commercial dies.

Note that even if none of the candidate constitutive equations fulfills the desired degree of accuracy, some information can still be drawn to help in the selection of better models or the reorientation of the characterization experiments.

3 Materials and methods

3.1 Non-commercial 4-channel extrusion die

The proposed methodology requires the manufacturing of an easy-to-build 4-channel extrusion die with lower geometric

complexity (Fig. 1b) than those manufactured for commercial purposes. The die extrudes four circular-shaped profiles with the following diameters (in mm): 6, 8, 10, and 12. Circular-shaped channels allow high-quality extrudate products for a wide range of rubbers and operation conditions [4]. This makes easier and more objective the validation based on the percentage of total flow that goes through each channel. The circular-shaped geometry ensures the generalization capacity of the simulation results. Hence, the extrusion conditions in terms of viscosity and local shear rate are similar to extrusion dies of commercial profiles.

Two plates compose the die: the extruder mounting plate (Fig. 1c) and the die land plate (Fig. 1d). The mounting plate is designed to conduce rubber from the inlet section to the entrance of the four exit channels at similar pressure values. The land plate needs enough depth to obtain a fully developed rubber flow at the exit of each channel. The extrusion die used in this research work was manufactured at the Standard Profil S.A. plant located in northern Spain.

3.2 Finite element model of the rubber extrusion die

Finite element (FE) analysis of extrusion die is performed using the commercial CFD solver Ansys Polyflow 14.0 [35] run on an Intel Xeon® Processor E5410 (12 MB cache, 2.33 GHz, 1333 MHz FSB). The software implements the FEM [21] instead of the FVM [36] to solve the governing equations and also includes packages for modeling generalized Newtonian fluid (GNF).

The system of governing equations is comprised by momentum (Navier-Stokes, Eq. 1) and mass conservation (Eq. 2) equations [37]. Energy equations are excluded as isothermal flow is assumed leaving the governing equations as follows:

$$\rho \frac{D\overrightarrow{V}}{Dt} = \overrightarrow{f} + \overrightarrow{\nabla} \cdot \sigma_{ij} \tag{1}$$

$$\frac{\delta\rho}{\delta t} + \overrightarrow{\nabla} \cdot \left(\rho \overrightarrow{V} \right) = 0 \tag{2}$$

where ρ is the density, $\overrightarrow{V}$ is the velocity vector, $\overrightarrow{f}$ is the volume forces, σ_{ij} is the stress tensor, and t is the time. Several assumptions, on the basis of the conditions met by the extrusion process, are undertaken to simplify the initial governing Eqs. 1 and 2 and the speed computations:

- Extrusion is modeled as a steady process excluding extruder start-up and shutdown phases.
- Rubber compounds can be considered incompressible fluids due to their high viscosity. Creeping flow assumption is also imposed because of the low Reynolds value ($Re \ll 0$). Consequently, inertia terms are neglected, and density is not required to solve the governing equations.

- Gravity terms are ignored as volume force given the small die dimensions.
- Additional volume or surface forces are not considered.

According to these conditions, a governing Eqs. 1 and 2 are simplified as follows:

$$-\overrightarrow{\nabla}P + \overrightarrow{\nabla} \cdot \tau_{ij} = 0 \tag{3}$$

$$\overrightarrow{\nabla} \cdot \overrightarrow{V} = 0 \tag{4}$$

where P is the pressure, and τ_{ij} is the viscous stress tensor. Here, the constitutive equations are required to relate the viscous stress tensor (τ_{ij}) to the strain rate tensor $\left(\dot{\gamma}_{ij}\right)$, which can be ultimately expressed in terms of the velocity components (u, v, w) making the system solvable.

$$\tau_{ij} = f\left(\dot{\gamma}_{ij}\right) \tag{5}$$

where the function f depends on the rubber behavior during the extrusion that varies from the simple linear relation of Newtonian models to the more complex equations of viscoelastic or time-dependent fluids.

Concerning the domains of the extrusion die, half of the die is simulated due to the symmetry condition (Fig. 2). The boundary conditions imposed in each domain are as follows:

- Inlet (1): Flow rate is established following experimental results. Fully developed flow condition is assumed in order to define the shape of the velocity profile.
- Symmetry plane (2): $f_s = 0$, $v_n = 0$.
- Outlet (3): Channels are long enough to consider fully developed flow condition: $f_n = 0$, $v_s = 0$.
- Walls (4): Non-slip condition at die walls ($v_s = 0$, $v_n = 0$).

The final FE model geometry (Fig. 3) corresponds to the dimensions of the manufactured die. Different types of mesh
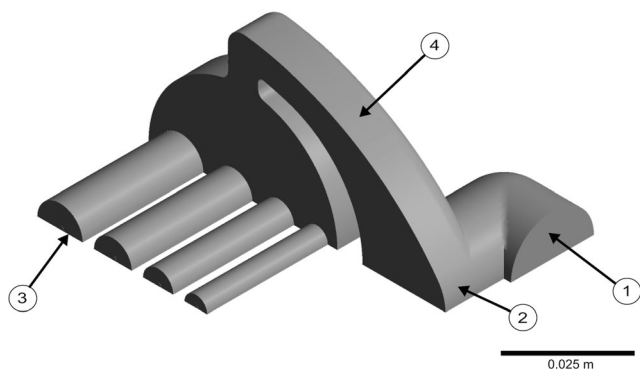
Fig. 2 Fluid domain for the simulations making use of symmetry to reduce computational requirements: inlet (*1*), symmetry plane (*2*), outlet (*3*), and walls (*4*)

0.015 m
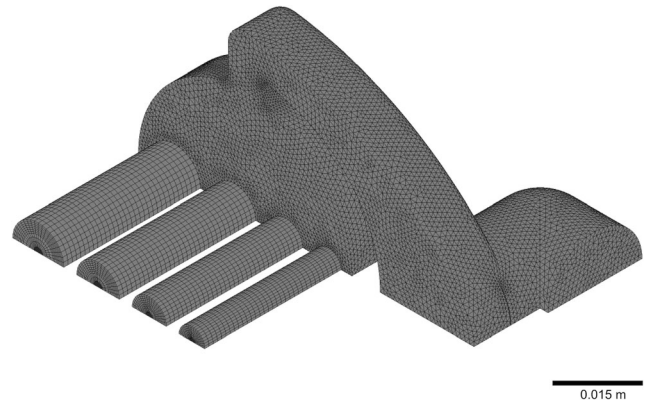
Fig. 3 Overview of the meshed FE model of the proposed extrusion die with two gates (making use of symmetry to reduce computational requirements). Hexahedral elements are used for the exit channels and rest of the domain is meshed using tetrahedral elements

are generated with Ansys Meshing [38], and mesh independency of the solution is examined in preliminary simulations [39]. The equivalency between mesh solutions obtained with hexahedral and tetrahedral meshes with distinct maximum element sizes has also been verified. The four exit channels are meshed using a sweeping technique with hexahedral elements, while the rest of the die is meshed with tetrahedral elements (maximum element size 5 μm). The interpolation functions used in both types of meshing are the same: constant value for pressure and mini-element approach for velocity. The final mesh is composed of 301,422 elements with the best balance between computation costs and accuracy.

3.3 Rheological characterization and constitutive curves

The tested material used for validating the methodology proposed was a particular EPDM produced by Standard Profil S.A. (labeled as EPDM-917). As compressibility is neglected, the kinematics of the EPDM-917 was modeled as a particular subtype of non-Newtonian models, a GNF [15]. These kind of fluids experiment a non-linear variation of viscosity η for different shear rate values $\dot{\gamma}$:

$$\eta = g(\dot{\gamma}) \tag{6}$$

where the function g is the viscosity curve or equation, and $\dot{\gamma}$ is the magnitude of the strain rate tensor γ_{ij}. Under shear flow conditions, this magnitude is referred as shear rate, and it depends on the second invariant of the strain rate tensor as follows:

$$\dot{\gamma} = \sqrt{\frac{1}{2}\left(\dot{\gamma}_{ij} : \dot{\gamma}_{ij}\right)} \tag{7}$$

The constitutive characterization of the EPDM-917 was performed by using an experimental program at the "Instituto Tecnológico de Aragón" located in Spain. Three

different rheological tests were performed based on different characterization techniques. Three viscosity models (one per series of experiments) were subsequently fit to the experimental data recorded and selected as candidates to approximate the experimental data: Herschel-Bulkley (HB), power law, and Bird-Carreau (BC).

The first candidate model was Herschel-Bulkley (HB) [40, 41], and the constitution equation could be expressed as follows:

$$\eta = \frac{\tau_0}{\dot{\gamma}} + K\dot{\gamma}^{n-1} \tag{8}$$

where τ_0 is the yield stress, K is the viscous parameter, and n is the power index. Coefficients of the Eq. 8 were derived from the experimental data recorded with a dynamic mechanical analysis (DMA) +450 rheometer (Metravib). Two tests were performed based on the squeeze flow theory [42]: a creep test for determining τ_0 and a compression test for obtaining K and n. Disks of 5.720 mm height and 5.970 mm radius were used for both experiments. The creep test was executed at a constant squeezing force of 75 N at 80 °C. A value of 47,062 Pa for τ_0 was obtained based on the following expression:

$$\tau_0 = \frac{3}{2}\frac{F}{\pi R_0^3}\frac{H_\infty^{5/2}}{H_0^{3/2}} \tag{9}$$

where F is the squeezing force, R_0 and H_0 are the initial dimensions of the disk, and H_∞ is the final height after the test, in this case 1.710 mm. The compression test was performed at constant squeezing rate at 80 °C, and both the force required F and the plate separation H were measured (Fig. 4).
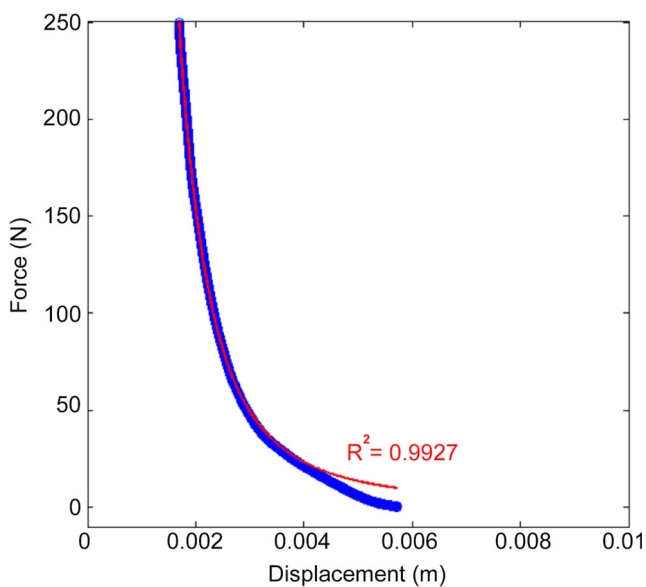
Fig. 4 Squeezing force F and plate separation H recorded during the compression test (*blue line*). The fitted curved is shown in *red*

Then, a curve was fit by ordinary least squares to the values of F and H recorded based on the next expression, which relates F and H [20].

$$F = \frac{2\pi R^3}{3H}\tau_0 + \frac{2\pi R^3}{(n+3)H}K\left(\frac{2n+1}{n}\right)^n\left(\frac{RV}{H^2}\right)^n \tag{10}$$

where R is the radius of the plates, τ_0 is the yield stress from in the creep test, and V is the set squeeze rate. HB parameters obtained based on this fit were 1 for n and 1.9059×10^7 Pa s for K, with a coefficient of determination (R^2) of 0.9927.

The second model was the power law by Ostwald and De Waele [17]:

$$\eta = K\dot{\gamma}^{n-1} \tag{11}$$

where K is the viscous parameter or consistency factor and n is the power law index. The curve was determined by a series of experiments performed with the EPDM in the non-commercial 4-channel extrusion die at Standard Profil S.A. plant. The power index n was obtained with the following expression:

$$n = \frac{1}{\dfrac{ln\left(\dfrac{Q_i}{Q_j}\right)}{ln\left(\dfrac{R_i}{R_j}\right)} - 3} \tag{12}$$

where Q is the flow going through each channel, and R is the channel radius. This expression is a simplification of the fluid equations when the rubber flows through two channels (i and j) of different diameter. As the proposed die is composed of four channels (Fig. 1b), six different pairs of channels with different radius could be made, and six distinct power law indexes were computed. The mean value ($n = 0.53$) was selected for the power law model. Regarding the viscous parameter K, and on the basis of previous experiences and experiments of Standard Profil S.A., a value of 15,283 Pa s was adopted in this study.

The third model was Bird-Carreau (BC) [40], a variation of the power law with two plateaus at high and low shear rates:

$$\eta = \eta_\infty + (\eta_0 - \eta_\infty)\left(1 + \lambda^2\dot{\gamma}^2\right)^{\frac{n-1}{2}} \tag{13}$$

where η_0 and η_∞ are the plateaus at zero and infinite shear rates, λ is the relaxation time or viscous parameter, and n is the power index. The central part of the curve, which exhibits a linear dependence between viscosity and shear rate, can be obtained by DMA in a DMA +450 rheometer (MetraviB). This test provides λ and n, i.e., the height and slope of the linear part of the BC curve. The DMA test can be used to characterize viscoelastic materials, though the elastic part in

this case was later depreciated. It works as follows. Rubber disks of 5 mm height and 10 mm diameter were placed between two circular plates. The lower plate was sinusoidally oscillated, while a torsional strain-measuring device was placed in the upper plate to detect the response of the material in terms of shear stress and the phase difference between upper and lower plates. The oscillation frequency on the lower plate varied between 0.1 to 100 Hz. The test was repeated at different temperatures (60, 70, 80, 90, 100, 110, and 120 °C) and the responses recorded (Fig. 5a.).

Then, all responses were shifted in time to a reference temperature of 120 °C, extending the frequency range from $10^{-1} - 10^{3}$ to $10^{-2} - 10^{5}$ Hz. Afterwards, the response of the material was expressed in terms of the in-phase or storage modulus

(G') and the out-of-phase or loss modulus (G"). G' measures the elastic response of the material while G" quantifies the viscous part. From G" and G' curves, the real (η') and the imaginary (η'') parts of the complex viscosity (η^*) (Fig. 5b) were obtained based on the following equality:

$$\eta^* = \frac{G^*}{\omega} = \frac{G'}{\omega}sin(\omega t) + \frac{G''}{\omega}cos(\omega t)$$
$$= \eta'' sin(\omega t) + \eta' cos(\omega t) \tag{14}$$

The complex viscosity-frequency profile can be correlated to the apparent viscosity-shear rate profile for some materials based on the Cox-Merz relationship [7]. Hence, the apparent viscosity curve was straightforwardly obtained. As aforementioned,

Fig. 5 Surface stress (K) and phase difference between upper and lower plates (d k) recorded during the dynamic mechanical analysis at different oscillation frequencies (a). Real (η') and imaginary (η'') components of complex viscosity (η^*) derived from **a** after time-temperature superposition (b)
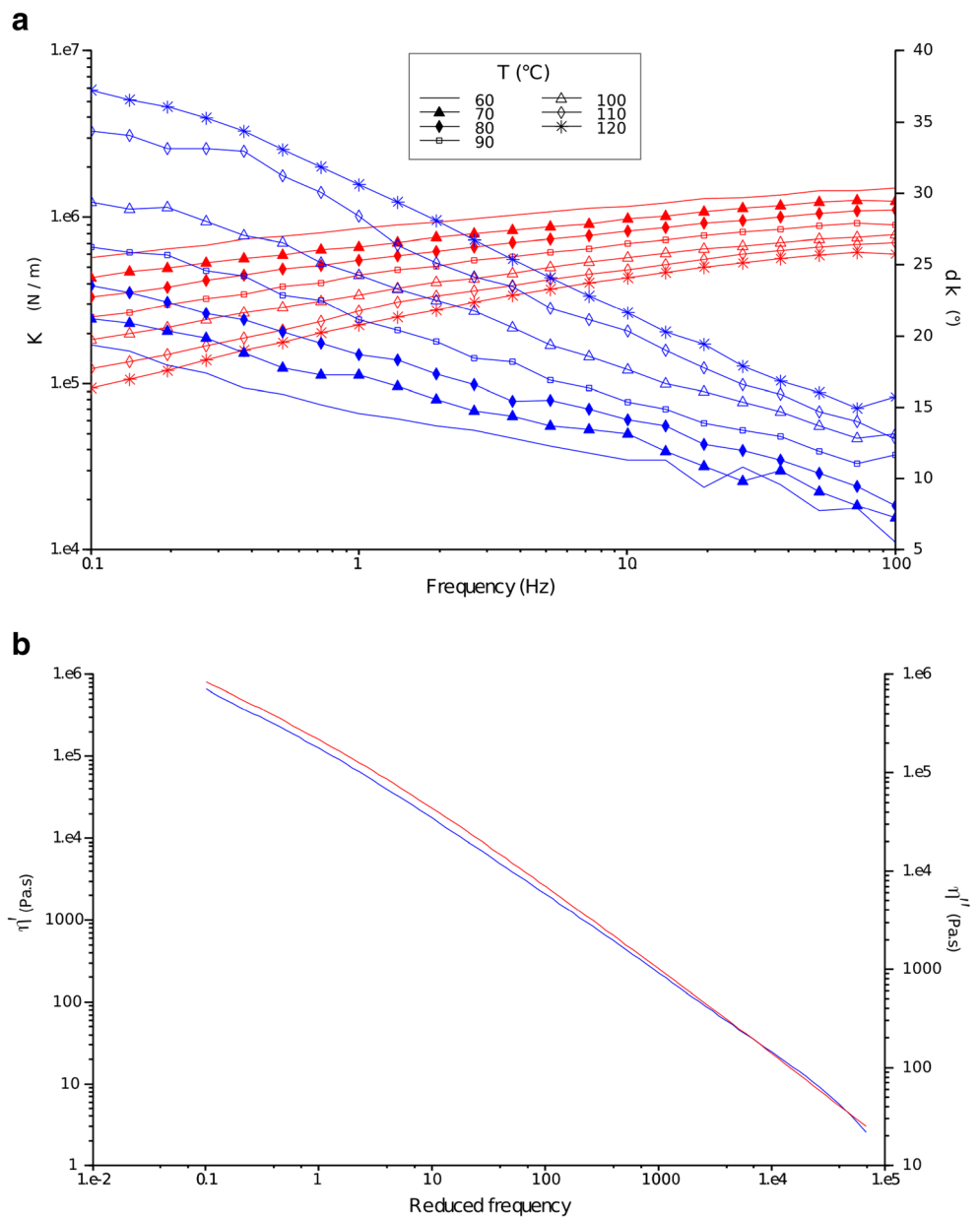
complex viscosity η^* was reduced to its real part η' as all elastic effects were neglected in simulations. The final viscosity curve was approximated by a linear curve (power law model) with n coefficient of 0.1562 and λ value of $5 \times 10^5 \, s$.

In regard to both plateaus, η_0 was maintained at the same value as in the Herschel-Bulkley model at 10^{10} Pa s, and η_∞ was set at 50 Pa s by performing additional tests with a capillary rheometer [43].

The three viscosity models fitting with the experimental data are summarized in Fig. 6 and Table 1. Power law curve is less complex than HB and BC from the characterization point of view as the model assumes a constant variation of viscosity and local shear rate and discards the maximum and minimum plateaus. Power law is also the most straightforward constitutive curve as profile manufacturers can easily carried out the necessary experiments without any external support and assistance.

The second model, the HB constitutive curve, requires specific equipment for calibration. HB includes the plateau of high shear rate in contrast to the power law, while the slope for the linear zone is steeper. The third model, the Bird-Carreu curve, shows the most complex characterization performed by DMA providing a curve with a similar slope to the power law but with two plateaus at the edges. BC is able to undertake the realistic modeling of rubber extrusion processes at higher shear rates than HB and power law models.

3.4 Experimental program for the 4-channel extrusion die

Several experimental tests with the EPDM-917 were performed with the proposed 4-channel extrusion die at the Standard Profil S.A. production plant. Processing parameters were established by plant operators given parameters' wide use in diverse rubber products. Rubber was extruded five times during 30 s at extruder rate of 30 rpm. Once finished, the extrudate of every channel was cut and weighed to obtain the average of mass rate per channel and
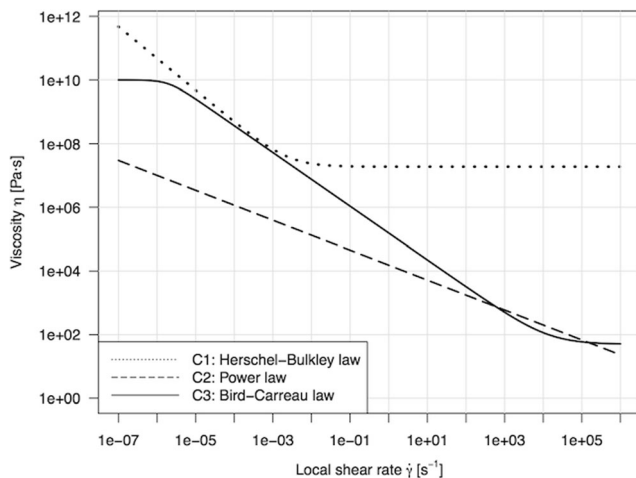
Fig. 6 Representation of the three viscosity models for the EPDM-917 estimated from the experimental data collected in three characterization tests

Table 1 Summary of the coefficients of the three viscosity models for the EPDM-917 estimated from the experimental data

Name	Coefficient	Value	Units
Herschel-Bulkley law	τ_0	47,062	Pa
	n	1	–
	K	1.9059×10^7	Pa s
Power law	n	0.53	–
	K	15,283	Pa s
Bird-Carreu law	n	0.1562	–
	λ	5×10^5	s
	η_0	10^{10}	Pa s
	η_∞	50	Pa s

percentage of the total flow leaving each channel (Table 2). Inlet die pressure P_{IN} was also recorded, averaging 15 MPa throughout all the experiments. Finally, the local shear rate $\dot{\gamma}$ at the extrusion die was known to vary between 10^{-3} and $10^1 \, s^{-1}$ during the extrusion process.

Note that the percentage of flow leaving each channel is the principal variable employed for the validation process of simulations, but P_{IN} and $\dot{\gamma}$ are also included to gain deeper insight into simulation results.

4 Results and discussion

Three CFD simulations based on the governing equations and boundary conditions described on Section 3.2 were run using the three constitutive models approximated (Section 3.3). The adequacy of each constitutive model was evaluated by the percentage of the total flow leaving each channel and the total inlet pressure (Table 3). Simulations of BC model showed the best agreement with experiments with the greatest difference between predicted and real flow around 2 % in channel 1. In contrast, flow distributions using HB and power law models (Fig. 7) were far from empirical values in channels 1, 3, and 4. Regarding die pressure, computed inlet pressure P_{IN} was 15.3 MPa for the viscosity BC model (Fig. 8c), close enough to the experimental value (15 MPa). However, the pressure at die inlet fell out of the expected range for the HB model and the power law with a value of

Table 2 Diameters of the channels and average values of the experimental flow distribution per channel

|	$\dot{M}$ [g/s]	% of total flow	Diameter [mm]
Channel 1	9.308	68.1	12
Channel 2	3.940	28.8	10
Channel 3	0.394	2.9	8
Channel 4	0.024	0.2	6
Total	13.665	100	

Table 3 Flow distribution per channel ($\dot{M}_i$) and inlet pressure (P_{IN}) measured from the experimental tests and obtained from the CFD simulations performed using the three viscosity curves

|	$\dot{M}_1$ [%]	$\dot{M}_2$ [%]	$\dot{M}_3$ [%]	$\dot{M}_4$ [%]	P_{IN}[MPa]
Experiment	68.1	28.8	2.9	0.2	15
Herschel-Bulkey law	55.8	28.2	11.9	3.8	28,690
Power law	58.9	28.0	10.1	2.6	5
Bird-Carreau law	66.4	28.0	4.8	0.4	15.3

28,690 and 5 MPa, respectively. These results demonstrate that the BC model was the appropriate constitutive equation for modeling the EPDM-917 behavior under the particular conditions of the studied extrusion process. Consequently, BC model could be considered a good candidate curve for defining EPDM-917 in future CFD simulations of commercial dies under similar extrusion conditions.

Once the most adequate constitutive equation was identified as BC curve, the simulations with the remaining models (HB and power law) were deeply analyzed. Although the differences between the candidate models were wide in this study, this may situation not be the case when working with other compounds or using similar characterization techniques. Moreover, a valid model may not be initially available, so there would be a need to redirect the experiments. Hence, the strength of proposed methodology when dealing with non-proper viscosity models needed to be evaluated.

Herschel-Bulkley model generated significant differences between experiments and simulations. The percentage of total flow leaving the channel 1 showed an average difference greater than 12 % between experimental and simulation results. The pressure at the die inlet in simulations P_{IN} was 28,690 MPa (Fig. 8a). This P_{IN} value is surprisingly much higher than the average of measured pressures (15 MPa), even
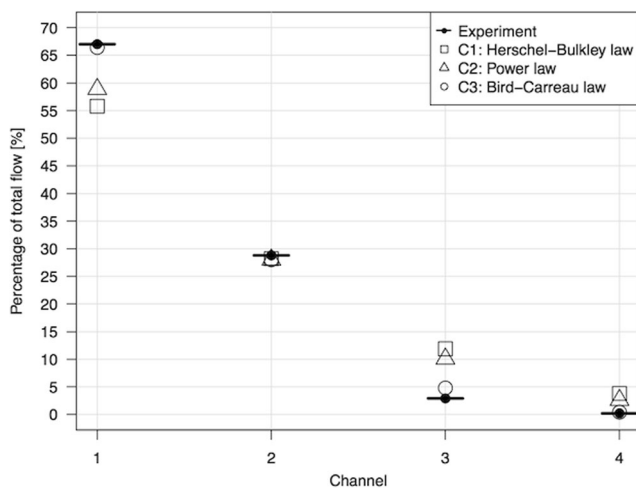

Fig. 7 Graphical comparison of the flow distribution per channel computed by CFD simulations against the experimental data
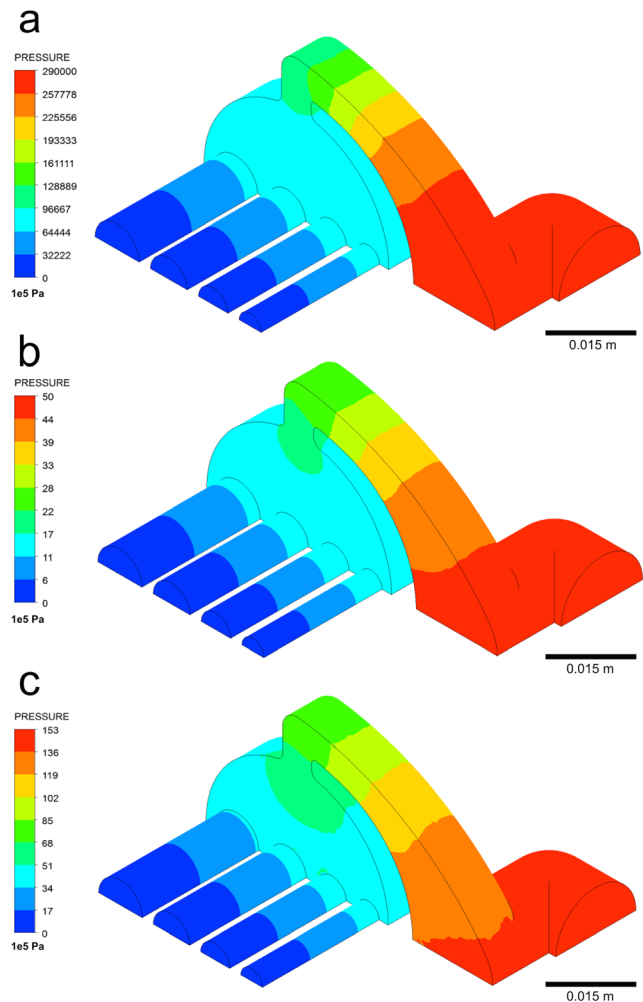
Fig. 8 Pressure contour plots obtained using **a** Herschel-Bulkley equation, **b** power law, and **c** Bird-Carreau equation

if pressure distribution in HB model had similar appearance to the simulations using BC model (Fig. 8). This could be explained by looking at the governing equations of the CFD model (Eq. 3). According to the model assumptions, the Navier-Stokes equations balance the effects of pressure and viscosity. An increment in viscosity increases pressure; hence, an upward displacement of the viscosity of HB model produced an increase in pressure values. Viscosity values were excessively high in the shear rate range where extrusion primarily takes place $\left(10^{-3}\ \mathrm{s}^{-1} < \dot{\gamma} < 10^{1}\ \mathrm{s}^{-1}\right)$. The inadequacy of the viscosity curve was explained by the nature of the characterization performed with the DMA squeeze flow test. This experiment was run at very low shear rate $(\dot{\gamma} < 10^{-2}\ \mathrm{s}^{-1})$ due to technical limitations related to the testing equipment, and the Newtonian plateau at high shear rates was created by extrapolation. Since the extrapolated plateau fell into the extrusion shear rate range, the errors increased sharply providing straightforward evidence that the experimental range of shear rate was not correctly established. Rather than exhibiting a plateau, the curve should have maintained a decreasing trend
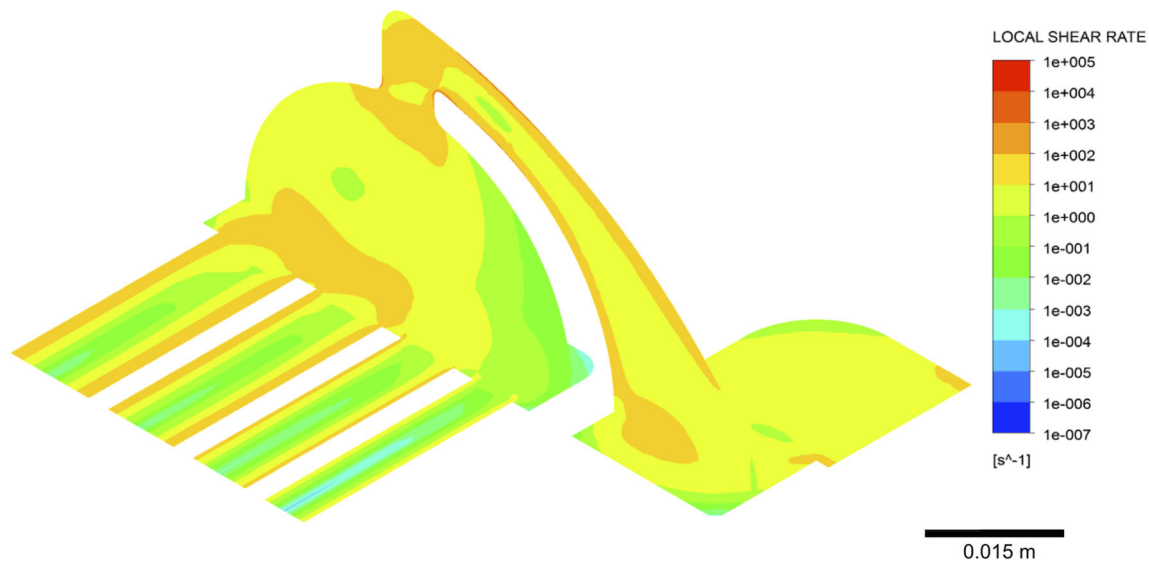
Fig. 9 Local shear rate contour plot obtained from the simulation results with the validated Bird-Carreau constitutive equation

to accurately predict the rubber behavior. Consequently, we demonstrate that the squeeze flow theory was not the adequate approach to characterize the EPDM-917 under the operation conditions of the extrusion line.

The use of the power law did not generate the expected flow distribution in the CFD model. A 9 % error in the percentage of the total flow leaving channel 1 was reported with the same tendency shown in HB model simulations: the predicted flow was higher than the real flow in small diameter channels while the opposite occurs in large diameter channels (Fig. 7 and S1). By contrast, a pressure P_{IN} of 5 MPa was obtained, which did not match the experimental value (15 MPa), but it is more acceptable than the value obtained using the HB model. The problem with the power law here was linked to the slope of the viscosity curve, provided by the power law exponent n and the flow distribution obtained. As depicted in Fig. 9, local shear rate increased proportionally to the channel diameter. Therefore, if the slope of the viscosity curve was not steep enough, the viscosity would increase in the channels of low shear rate (channel 4) while it would decrease in the channels of high shear rate (channels 1 and 2). As viscosity is directly related to flow resistance, this explained the flow distribution observed in Table 3 and Fig. 7. To solve this problem, the power law slope should be steeper by decreasing n in order to add resistance in channels 3 and 4 and increase the flow through channel 1.

We demonstrated that combining the 4-channel die and the methodology proposed allows us to explain important differences between experimental results and simulations and draw some conclusions. In view of simulation results derived from the HB model, the range of the shear rate in the characterization tests using DMA +450 equipment should be extended

$(10^{-3} \text{ s}^{-1} < \dot{\gamma} < 10^1 \text{ s}^{-1})$. The analysis of the power law simulation results shows that n coefficient (steeper slope) should be smaller for the interval of the curve that follows the power law. This is related to the design of the 4-channel die for characterizing rubber compounds using Eq. 12; thus, future geometry modifications of the die are required to correct this issue. The complete analysis would allow guiding future characterization experiments when none of existing viscosity curves was adequate enough. However, in this study, no additional models are required because the BC model already fulfills our demands.

5 Conclusions

A new methodology is proposed to help in the selection of the appropriate constitutive curve of rubber blends for simulating the extrusion process of complex profiles. This selection cannot be easily done "a priori" due to the wide variety of constitutive equations available. Our methodology, based on combining CFD simulations and a series of experiments using an easy-to-build non-commercial 4-channel die, was successfully validated with a particular EPDM produced by Standard Profile S.A. (labeled as EPDM-917). From three candidate constitutive models, our method showed Bird-Carreau as the most appropriate constitutive model to simulate the extrusion process of EPDM-917 under particular operating conditions. This research work represents a step forward in the integration of CFD simulations in the design phase of extrusion dies for long rubber profiles. Profile manufacturers will better face the simulation of their commercial profiles once the constitutive curves for their rubber blends are successfully validated.

References

1. Cho JR, Choi JH (2016) Numerical investigation of weather strip extrusion forming process by thermal flow analysis. Int J Adv Manuf Technol :1–11

2. Marcos González A, Pernía Espinoza AV, Alba Elías F et al (2007) A neural network-based approach for optimising rubber extrusion lines. Int J Comput Integr Manuf 20(8):828–837

3. Li Y, Yang H, Xing Z (2016) Numerical simulation and process optimization of squeeze casting process of an automobile control arm. Int J Adv Manuf Technol :1–7

4. Milivoje MK, Louis GR (2007) Design of extrusion dies. In: Encyclopedia of Chemical Processing, vol null. vol null. Taylor & Francis, pp 633–649

5. Gonçalves ND, Carneiro OS, Nóbrega JM (2013) Design of complex profile extrusion dies through numerical modeling. J Non-Newtonian Fluid Mech 200(0):103–110

6. Singhry HB, Abd Rahman A, Imm NS (2015) Effect of advanced manufacturing technology, concurrent engineering of product design, and supply chain performance of manufacturing companies. Int J Adv Manuf Technol :1–7

7. Cox WP, Merz EH (1958) Correlation of dynamic and steady flow viscosities. J Polym Sci 28(118):619–622

8. Liu P, Shuisheng X, Cheng L (2012) Die structure optimization of large, multi-cavity aluminum profile using numerical simulation and experiments. Mater Des 36:152–160

9. Martínez de Pisón FJ, Barreto C, Pernía Espinoza AV et al (2008) Modelling of an elastomer profile extrusion process using support vector machines (SVM). J Mater Process Technol 197(1–3):161–169

10. Elgeti S, Probst M, Windeck C et al (2012) Numerical shape optimization as an approach to extrusion die design. Finite Elem Anal Des 61(0):35–43

11. Michaeli W (1992) Extrusion dies for plastic and rubber: design and engineering computations, 2nd edn. Hanser Gardner Publications, Munich

12. Mu Y, Zhao G, Chen A et al (2013) Modeling and simulation of polymer melts flow in the extrusion process of plastic profile with metal insert. Int J Adv Manuf Technol 67(1):629–646

13. Mu Y, Zhao G, Wu X et al (2010) An optimization strategy for die design in the low-density polyethylene annular extrusion process based on FES/BPNN/NSGA-II. Int J Adv Manuf Technol 50(5):517–532

14. Barreto Cabrera C, Ordieres Meré J, Castejón Limas M et al (2010) A data-driven manufacturing support system for rubber extrusion dies. Int J Prod Res 48(8):1–13

15. Dafermus C, Ericksen JL, Kinderlehrer D (1987) Amorphous polymers and non-Newtonian fluids. Springer, New York, NY

16. Siegbert R, Yesildag N, Frings M et al (2015) Individualized production in die-based manufacturing processes using numerical optimization. Int J Adv Manuf Technol 80(5):851–858

17. Ostwald W (1925) Concerning the function rate of the viscosity of dispersion systems. Kolloid Zeitschrift 36:248–150

18. Liang JZ (1996) A study of the die-swell behaviour of rubber compounds during short-die extrusion. J Mater Process Technol 59(3):268–271

19. Sienz J, Goublomme A, Luege M (2010) Sensitivity analysis for the design of profile extrusion dies. Comput Struct 88(9–10):610–624

20. Meeten GH (2002) Constant-force squeeze flow of soft solids. Rheol Acta 41:557–566

21. Zienkiewicz OC, Taylor RL, Zhu JC (2005) The finite element method for fluid dynamics, 6th edn. Butterworth-Heinemann, Oxford

22. del Coz Díaz JJ, García Nieto PJ, Bello García A et al (2008) Finite volume modeling of the non-isothermal flow of a non-Newtonian fluid in a rubber's extrusion die. J Non-Cryst Solids 354(47–51):5334–5336

23. del Coz Díaz JJ, García Nieto PJ, Ordieres Meré J et al (2007) Computer simulation of the laminar nozzle flow of a non-Newtonian fluid in a rubber extrusion process by the finite volume method and experimental comparison. J Non-Cryst Solids 353(8–10):981–983

24. Vaddiraju SR, Kostic M, Reifschneider L et al. (2004) Extrusion simulation and experimental validation to optimize precision design dies. In: ANTEC 2004-Annual Technical Conference Proceedings, Chicago, IL. Society of Plastics Engineers, pp 76–80

25. Carneiro OS, Nóbrega JM, Pinho FT et al (2001) Computer aided rheological design of extrusion dies for profiles. J Mater Process Technol 114(1):75–86

26. Ha YS, Cho JR, Kim TH et al (2008) Finite element analysis of rubber extrusion forming process for automobile weather strip. J Mater Process Technol 201(1–3):168–173

27. Ganvir V, Lele A, Thaokar R et al (2009) Prediction of extrudate swell in polymer melt extrusion using an Arbitrary Lagrangian Eulerian (ALE) based finite element method. J Non-Newtonian Fluid Mech 156(1–2):21–28

28. Mitsoulis E, Georgiou GC, Kountouriotis Z (2012) A study of various factors affecting Newtonian extrudate swell. Comput Fluids 57(0):195–207

29. Edwards KL (1998) A designers' guide to engineering polymer technology. Mater Des 19:57–67

30. Mompean G, Thais L, Tomé MF et al (2011) Numerical prediction of three-dimensional time-dependent viscoelastic extrudate swell using differential and algebraic models. Comput Fluids 44(1):68–78

31. Pauli L, Behr M, Elgeti S (2013) Towards shape optimization of profile extrusion dies with respect to homogeneous die swell. J Non-Newtonian Fluid Mech 200(0):79–87

32. Al-Muslimawi A, Tamaddon-Jahromi HR, Webster MF (2013) Simulation of viscoelastic and viscoelastoplastic die-swell flows. J Non-Newtonian Fluid Mech 191(0):45–56

33. Müllner HW, Eberhardsteiner J, Mackenzie-Helnwein P (2009) Constitutive characterization of rubber blends by means of capillary-viscometry. Polym Test 28(1):13–23

34. Müllner HW, Wieczorek A, Eberhardsteiner J (2011) Experimental determination of shear-thinning behaviour during extrusion of rubber blends. Strain 47(2):167–172

35. ANSYS I (2011) ANSYS POLYFLOW User's Guide, 14th edn. ANSYS, Inc, Canonsburg, PA

36. Versteeg H, Malalasekera W (2007) An introduction to computational fluid dynamics: the finite volume method, 2nd edn. Pretince Hall

37. Cengel YA, Cimbala JM (2006) Fluid mechanics: fundamentals and applications, 2nd edn. McGraw-Hill, New York, NY

38. ANSYS I (2011) ANSYS Meshing user's guide, 14th edn. ANSYS, Inc, Canonsburg, PA

39. del Coz Díaz JJ, García Nieto PJ, Suarez Sierra JL et al (2013) Nonlinear thermal optimization of external light concrete mulit-

holded brick walls by the finite element method. Int J Heat Mass Transf 51:1530–1541

40. Chhabra RP (2010) Non-Newtonian fluid: an introduction. In: Deshpande AP, Krishnan JM, Kumar S (eds) Rheology of complex fluids. Springer, New York, NY

41. Zhu H, Kim YD, De Kee D (2005) Non-Newtonian fluids with a yield stress. J Non-Newtonian Fluid Mech 129(3):177–181

42. Smyrnaios DN, Tsamopoulos JA (2001) Squeeze flow of Bingham plastics. J Non-Newtonian Fluid Mech 100:165–190

43. Jones DS (1999) Dynamic mechanical analysis of polymeric systems of pharmaceutical and biomedical significance. Int J Pharm 179(2):167–178